Title

Genetic Disruption of Circadian Rhythms in the Suprachiasmatic Nucleus Causes Helplessness, Behavioral Despair, and Anxiety-like Behavior in Mice

Journal

Biological Psychiatry, 80(11)

ISSN

0006-3223

Authors

Landgraf, Dominic
Long, Jaimie E
Proulx, Christophe D
et al.

Publication Date

2016-12-01

DOI

10.1016/j.biopsych.2016.03.1050

Peer reviewed

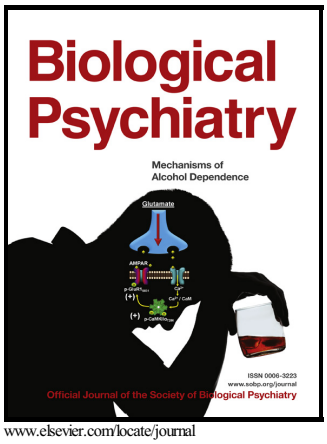

www.elsevier.com/locate/journal

Genetic Disruption of Circadian Rhythms in the Suprachiasmatic Nucleus Causes Helplessness, Behavioral Despair, and Anxiety-Like Behavior in Mice

Dominic Landgraf, Jaimie E. Long, Christophe D. Proulx, Rita Barandas, Roberto Malinow, David K. Welsh

PII: S0006-3223(16)31101-5
DOI: http://dx.doi.org/10.1016/j.biopsych.2016.03.1050
Reference: BPS12835

To appear in: *Biological Psychiatry*

Received date: 11 September 2015
Revised date: 4 March 2016
Accepted date: 4 March 2016

Cite this article as: Dominic Landgraf, Jaimie E. Long, Christophe D. Proulx, Rita Barandas, Roberto Malinow and David K. Welsh, Genetic Disruption of Circadian Rhythms in the Suprachiasmatic Nucleus Causes Helplessness, Behavioral Despair, and Anxiety-Like Behavior in Mice, *Biological Psychiatry,* http://dx.doi.org/10.1016/j.biopsych.2016.03.1050

Genetic Disruption of Circadian Rhythms in the Suprachiasmatic Nucleus Causes Helplessness, Behavioral Despair, and Anxiety-Like Behavior in Mice

Dominic Landgraf[1, 2, *], Jaimie E. Long[1, 2], Christophe D. Proulx[3], Rita Barandas[1, 2, 4, 5], Roberto Malinow[3] & David K. Welsh[1, 2]

[1]Veterans Affairs San Diego Healthcare System, San Diego, CA

[2]Department of Psychiatry, and Center for Circadian Biology, University of California, San Diego, La Jolla, CA

[3]Department of Neurosciences, University of California, San Diego, La Jolla, CA

[4]Department of Psychiatry, Hospital de Santa Maria, Centro Hospitalar Lisboa Norte, Lisbon, Portugal

[5]Faculty of Medicine, University of Lisbon, Portugal

*Corresponding author: Dominic Landgraf, Department of Psychiatry, University of California, San Diego, 9500 Gilman Drive MC-0603, La Jolla, CA 92093-0603; e-mail: dolandgraf@gmail.com.

Short title: Disrupted Central Circadian Rhythms Cause Depression

Keywords: Circadian clocks, depression, suprachiasmatic nucleus, learned helplessness, corticosterone, mouse model

Abstract: 250 words

Article Body: 3984 words

Number of figures: 5

Number of tables: 0

Number of supplemental information: 5

Abstract

Background:

Major depressive disorder is associated with disturbed circadian rhythms. To investigate the causal relationship between mood disorders and circadian clock disruption, previous studies in animal models have employed light-dark manipulations, global mutations of clock genes, or brain area lesions. However, light can impact mood by non-circadian mechanisms, clock genes have pleiotropic, clock-independent functions, and brain lesions not only disrupt cellular circadian rhythms but also destroy cells and eliminate important neuronal connections, including light reception pathways. Thus, a definitive causal role for functioning circadian clocks in mood regulation has not been established.

Methods:

In this study, we stereotaxically injected viral vectors encoding shRNA to knock down expression of the essential clock gene *Bmal1* into the brain's master circadian pacemaker, the suprachiasmatic nucleus (SCN).

Results:

In these SCN-specific *Bmal1*-knockdown (SCN-*Bmal1*-KD) mice, circadian rhythms are greatly attenuated in the SCN, while the mice are maintained in a standard light/dark cycle, SCN neurons remain intact, and neuronal connections are undisturbed, including photic inputs. In the learned helplessness paradigm, these mice are slower to escape, even before exposure to inescapable stress. They also spend more time immobile in the tail suspension test and less time in the lighted section of a light/dark box. SCN-*Bmal1*-KD mice also show greater weight gain, an abnormal circadian pattern of corticosterone, and an attenuated increase of corticosterone in response to stress.

Conclusion:

Thus, disrupting SCN circadian rhythms is sufficient to cause helplessness, behavioral despair, and anxiety-like behavior in mice, establishing SCN-*Bmal1*-KD mice as a new animal model of depression.

Introduction

Our environment is characterized by recurring daily changes caused by the rotation of the earth. To optimally adjust their behavior, metabolism, and physiology to such predictable environmental changes, most living organisms evolved internal timekeeping systems, so-called circadian clocks. Cells of most tissues express clock genes in a ca. 24 hr rhythm. The hypothalamic suprachiasmatic nucleus (SCN) is the center of this clock network (1). The SCN regulates the period and the phase of all other clocks in the brain and the rest of the body and synchronizes them with the external light/dark cycle. However, neuronal pathways conveying retinal photic input also reach other brain regions, as well as peripheral tissues like the adrenal, and recent evidence suggests that these pathways may allow non-SCN clocks to remain synchronized even when the SCN clock is non-functional (2-6).

Major depressive disorder (MDD) and bipolar disorder are associated with disturbed circadian rhythms, indicated by disruptions of daily processes like sleep, appetite, and hormonal release (7-11) and weaker rhythms of clock gene expression in brains of MDD patients (12). However, whether disruptions of circadian clocks are causes or consequences of mood disorders remains elusive (13). Exposing rats to chronic mild stress to induce depression-like behavior reduces amplitude of locomotor activity, body temperature, and corticosterone rhythms (14, 15). In mice, chronic mild stress reduces circadian rhythm amplitude in the SCN and basolateral amygdala, but increases amplitude in the nucleus accumbens (16, 17). On the other hand, other studies suggest that circadian rhythm abnormalities may cause mood

disorders. In humans, environmental disruption of circadian rhythms, such as in shift work, increases the risk of depression (18). Mice with genetically disturbed circadian clocks often show depression- or manic-like behavior. However, due to pleiotropic, non-circadian functions of clock genes, mood phenotypes of such mice cannot be attributed unequivocally to circadian disruption. Moreover, clock gene mutations producing similar circadian phenotypes do not always produce similar mood-related phenotypes (13). Manipulating lighting conditions also leads to changes of both circadian and mood-related behavior (19). However, light/dark manipulations can have substantial impact on mood regulation independent of circadian clocks, e.g. by causing cell death or neurotransmitter switching of neurons in mood-regulating brain areas, or increased inflammatory factors (19-21). Lesions of the SCN lead to reduced behavioral despair (22). However, SCN lesions also destroy neurons and disrupt neuronal connections, including photic input pathways to other brain regions that have functions other than circadian rhythm regulation (23). In fact, SCN lesions can actually reverse the behavioral effects of SCN rhythm disruption in memory tasks, perhaps because an anatomically intact but dysrhythmic SCN produces an actively disruptive output signal (24).

In this study we present a mouse model with *Bmal1* shRNA-induced suppression of circadian rhythms restricted to the SCN. Since these mice developed normally, were kept under normal lighting conditions, and had intact light input pathways, intact SCN neurons and efferent connections, and intact molecular clocks outside the SCN, we can exclude many of the sorts of non-circadian effects caused by global knockouts of clock genes, light/dark manipulations, or SCN lesions. Our data reveal that selectively disturbing rhythms in the SCN master circadian pacemaker causes helplessness, behavioral despair, and anxiety-like behavior, as well as increased sensitivity to stress.

Materials and methods

Animals

All experiments were done in 8-14 week old male mPer2^{Luciferase} (PER2::LUC) mice. In PER2::LUC knockin mice, the wild type (WT) circadian clock gene *Period2 (Per2)* has been replaced by homologous recombination with a construct incorporating the firefly luciferase *(Luc)* gene in tandem with WT *Per2*, such that a bioluminescent PER2::LUC fusion protein is expressed under control of all *Per2* regulatory elements (25). In our mice, the reporter construct also incorporated an SV40 polyadenylation site to enhance expression levels (26), and mice were backcrossed to produce a congenic C57BL/6J background. Unless otherwise stated, mice were maintained in LD 12:12 cycles (12 h light, 12 h dark). Beginning 6 days before stereotaxic AAV injections, mice were single-housed with continuous access to water and food. We attempted to minimize the number of animals used and animal pain and distress. Mouse studies were conducted in accordance with regulations of the Institutional Animal Care and Use Committee at University of California, San Diego.

Virus production

To make cDNA encoding our small hairpin RNAs (shRNA) and suitable to produce adeno-associated virus (AAV) vectors, we first PCR amplified a sequence encoding the U6 promoter, the scrambled 19-nucleotide shRNA sequence, and the cytomegalovirus/green fluorescent protein (CMV/GFP) cassette from pLL3.7 vector (pLL3.7 Scr shRNA was a gift from Dr. Ulrike Heberlein, University of California, San Francisco [Addgene plasmid # 59299]) and subcloned it into the cDNA pAAV-DIO-ChR2(H134R)-eYFP (kindly provided by Dr. Karl Deisseroth, Stanford), using MluI and XhoI sites (the latter destroyed during cloning) to produce the vector pAAV-U6-SCRshRNA-CMV-GFP-WPRE. Sequencing confirmed gene

sequence integrity. Two 19-nucleotide shRNA sequences targeting *Bmal1* messenger RNA (GenBank: 11865) were kindly provided by Dr. Andrew C. Liu, University of Memphis: Bmal1-shRNA1 = 5'-GTCGATGGTTCAGTTTCAT and Bmal1-shRNA2 = 5'-GCATCGATATGATAGATAA. As controls we used two scrambled shRNAs (SCR-shRNA = 5'- GCGCTTAGCTGTAGGATTC from the vector pLL3.7 and the 19-nucleotide SCR2-shRNA = 5'-GCAACAAGATGAAGAGCAC) showing no significant alignment with any mouse mRNA. Complementary oligonucleotides encoding shRNAs were synthesized (Invitrogen, Grand Island, NY), annealed, and cloned in pAAV-U6-SCRshRNA-CMV-GFP-WPRE by ligation after HpaI and XhoI vector digestion.

Recombinant AAV-U6-SCR1shRNA-CMV-GFP, AAV-U6-SCR2shRNA-CMV-GFP, AAV-U6-Bmal1AshRNA-CMV-GFP and AAV-U6-Bmal1BshRNA-CMV-GFP were transfected into the 293A cell line (Invitrogen, Grand Island, NY) using the PEI transfection method along with the Ad helper vector pXX680 and a plasmid encoding capsid serotype 8. Then, 72h after transfection, 293A cells were collected and lysed by three freeze/thaw cycles. Recombinant AAVs from the cleared supernatant were purified on an iodixanol gradient and subsequently concentrated in an Amicon Ultra-4 centrifugal filter 50K device (Millipore, Billerica, MA, USA).

Virus injection

Mice were anesthetized with ketamine/dexmedetomidine in 0.9% saline (ketamine: 70 mg per kg body weight; dexmedetomidine: 0.3 mg per kg body weight) before bilateral stereotaxic injection of AAV particles in the SCN (anteroposterior: 0.46 mm posterior to bregma; mediolateral: 0.2 mm lateral to midline; dorsoventral: 5.5 mm below dura). About 0.5-0.8 µl of virus was injected into each position over ~30 min using a picospritzer (Parker). All mice received a mixture of two shRNAs: either both *Bmal1* or both scrambled shRNAs. To allow diffusion of the virus, the injection pipette remained immobile for 1

min before moving more ventral, and for 3 min before removing it. After surgery, mice were injected with 0.05 mg atipamezole for reversal of dexmedetomidine. Efficiency of *Bmal1*-KD was determined as described in supplemental materials.

Behavioral tests

To measure locomotor activity rhythms, SCN-*Bmal1*-KD and control mice were singly housed in running wheel-equipped cages, and locomotor activity was monitored under different lighting conditions. During the first 6 days, mice were maintained in LD 12:12 cycles (12 h light, 12 h dark) with light levels at 200 lux. Subsequently, mice were kept in constant darkness (DD) for 13 days. Sucrose preference, open field test, tail suspension test, and learned helplessness were performed as described previously (27). Detailed descriptions of these and other behavioral tests are provided in supplemental materials. Sucrose preference tests were performed twice per week with 1% sucrose water starting 6 days before AAV injections and continuing until mice were sacrificed at the end of all experiments. All other behavioral tests started three weeks after AAV injections to allow time for full expression of *Bmal1* shRNA. Testing began with the least stressful tests, followed by the more stressful tests, and finally the most stressful procedure, induction of learned helplessness.

Brain slice culture and PER2::LUC measurements

After all behavioral tests were complete, mice were anesthetized with isoflurane and killed by cervical dislocation, and organotypic SCN explants were prepared as described previously (28). PER2::LUC expression patterns were measured using a LumiCycle luminometer (Actimetrics, Wilmette, IL, USA) as described previously (28).

Blood sampling and corticosterone measurements

Details about the preparation of blood samples are provided in supplemental materials. Corticosterone concentrations were measured using a commercially available RIA kit (MP Biomedicals, Santa Ana, CA, USA). Plasma samples were diluted 1:200.

24-hour profile: Mice were transferred to a separate room 1 day before blood sampling began. Lights were turned off at the regular time of the LD 12:12 light/dark cycle, and then remained off until all blood samples were collected. Blood was sampled every four hours beginning at CT1 (7:00 AM) under dim red light. During sampling, mice were not restrained and were allowed to explore the bench area freely.

Restraint stress: To measure stress-related corticosterone release, mice were transferred to mouse restrainers (Plas Labs, Lansing, MI, USA) for 30 min. Blood was collected immediately before restraint stress (0 min), and after 10 min, 30 min, 60 min, and 90 min of restraint. All blood samples were collected between 6 and 9 hrs after lights on.

Data analysis

Statistical analyses were conducted using GraphPad Prism (GraphPad Software, La Jolla, CA, USA). Corticosterone release profiles were fit to Fourier curves with 2 harmonics using CircWave (developed by Roelof Hut, University of Groningen, Netherlands). Bioluminescence data were analyzed using LumiCycle Analysis software (Actimetrics, USA). Amplitude was determined over 5 days by fitting a sine wave [LM fit (Sin)] to 24 h running average baseline-subtracted data. In order to normalize amplitude to the size of cultured tissues, the sine wave amplitude was divided by the baseline bioluminescence brightness of each individual explant. The first day of measurement was excluded from analyses. Wheel-

running activity was analyzed using ClockLab software (Actimetrics, USA). The first 3 days of the DD condition were excluded from analysis. Data that were significant outliers ($p<0.05$) in the Grubb's test and >3 standard deviations from the mean of the remaining values were excluded. Details about statistical tests used for individual experiments are indicated in figure legends.

Results

SCN Bmal1-KD in vivo suppresses PER2::LUC rhythmicity in vitro

To test the effect of disrupted SCN clocks on mood-related behaviors in mice, we generated AAV vectors encoding shRNAs designed to target and downregulate *Bmal1* expression (Fig. 1A). The *Bmal1*-shRNA reduces BMAL1 protein levels by ~60% (Fig. 1B, C). After all behavioral experiments were completed, we sacrificed the animals and prepared organotypic SCN explants. We used these explants to confirm the correct injection site of the AAV particles and to determine the efficiency of the *Bmal1*-KD for each individual animal. The injection site was identified by the GFP reporter that was encoded by all of our AAV vectors (Fig. 1D, S1A, B). Animals that showed no GFP expression in the SCN were excluded from analyses (Fig. S1C). Reduced amplitude of PER2::LUC rhythms in SCN explants provided a quantitative estimate of the efficiency of *Bmal1* knockdown. In mice injected with *Bmal1* shRNA, amplitude of SCN PER2::LUC rhythms was decreased by ~80% and period was lengthened compared to control mice injected with scrambled sequence shRNA (Fig. 1E, F). Of ten mice with successfully targeted *Bmal1* shRNA, SCN rhythms were of drastically reduced amplitude in nine, and completely absent in one.

SCN-*Bmal1*-KD mice did not show GFP expression outside of the SCN, suggesting that non-SCN brain areas had intact molecular clocks (Fig. S2). To confirm that molecular clocks outside the SCN were not deficient, we cultured periaqueductal gray (PAG) explants from SCN-*Bmal1*-KD and control mice. The

PAG was shown previously to express stable circadian rhythms in culture (28). We found that PAG explants from SCN-*Bmal1*-KD mice and control mice were equally rhythmic (66.7% vs. 70% of slices rhythmic, n=12 and 10, respectively), indicating that molecular clocks in brain areas outside of the SCN were still functional despite SCN-specific *Bmal1*-KD.

To test effects of SCN-specific *Bmal1*-KD on behavioral rhythms, mice were transferred to DD to monitor the endogenous SCN-driven ("free-running") locomotor activity rhythm with running wheels. Like SCN explants from these mice, SCN-*Bmal1*-KD mice on running wheels exhibited a significantly longer circadian period compared to control mice, but did not show any other circadian locomotor rhythm abnormalities (Fig. 1G, H, S3).

To assess for possible tissue damage caused by the injection procedure or toxicity of shRNAs, injected and uninjected SCN explants were compared, and showed no differences in either histological appearance by bright field microscopy or amplitude of PER2::LUC rhythms. To assess for possible toxicity specific to *Bmal1* shRNA, SCN explants injected with *Bmal1* shRNA vs. scrambled sequence shRNA were compared, and showed no differences in either cell morphology or 24 hr mean level of PER2::LUC bioluminescence, which is an ATP-requiring enzymatic reaction requiring cell viability. Thus, injection of shRNAs did not adversely affect anatomical structure of the SCN or viability of SCN neurons. These results confirm that AAV-directed downregulation of *Bmal1* is sufficient to impair circadian rhythms in SCN and constitute a good model to test the impact of impaired SCN circadian rhythms on mood-related behavioral changes in mice.

Disrupting SCN rhythms causes helplessness, behavioral despair, anxiety-like behavior, and weight gain

Three weeks after the shRNA injections, mice underwent behavioral tests to determine the effects of disrupting SCN circadian rhythms on mood. Beginning six days before shRNA injection, we also performed a sucrose preference test twice a week in order to test for gradual changes in hedonic responses to sucrose (Fig. 2A). In the learned helplessness paradigm, reduced SCN rhythm amplitude induced by *Bmal1*-KD led to significant increases in escape latencies and number of escape failures (Fig. 2A). Mice with disrupted SCN rhythms also showed a significantly higher immobility time in the tail suspension test compared to control animals (Fig. 2B). In the light/dark box test, SCN-*Bmal1*-KD mice spent significantly less time in the light compartment (Fig. 2F), indicating increased anxiety-like behavior, but were not impaired in their spatial preference or total activity in the open field test (Fig. 2G).

Since mood disorders are often associated with metabolic disorders, we also tested weight gain and found that over the course of five weeks, SCN-*Bmal1*-KD mice gained significantly more weight than control mice (Fig. 2C). Knockdown of *Bmal1* in the SCN had no significant impact on preference for sweet sucrose water at any time point (sucrose preference test) (Fig. 2D), nor on the latency to approach and eat food in a novel environment (novelty-suppressed feeding test) (Fig. 2E). In this test, total food uptake was similar in SCN-*Bmal1*-KD and control mice.

Inescapable stress is not required for helpless behavior in SCN-Bmal1-KD mice

Because some mood-related behavior changes in SCN-*Bmal1*-KD mice were evident before IS, we investigated the importance of stress in more detail by testing for helplessness even in the absence of IS in a new group of SCN-*Bmal1*-KD and control mice. In these experiments, we tested active avoidance by performing only the testing phase of the learned helplessness paradigm, in which animals always had

the opportunity to escape. Even without any previous exposure to IS, SCN-*Bmal1*-KD mice displayed decreased active avoidance, with significantly longer escape latencies and more failures compared to control mice (Fig. 3). Thus, helplessness appears to develop spontaneously in SCN-*Bmal1*-KD mice. Importantly, when testing sensitivity to gradually increasing electric shock intensity, SCN-*Bmal1*-KD and control mice displayed no differences, demonstrating that the differences in active avoidance were not due to altered pain sensitivity (Fig. S4).

Stress response system is altered in SCN-Bmal1-KD mice

The circadian clock and the stress response system are closely related, and abnormal glucocorticoid levels are associated with the development of mood disorders (29). For this reason we investigated diurnal plasma corticosterone rhythms of SCN-*Bmal1*-KD and control mice under constant environmental conditions as well as corticosterone release in response to restraint stress. Control animals showed a single clear corticosterone peak at the beginning of their subjective night when they normally become active (25 hours after "lights off"). In contrast, SCN-*Bmal1*-KD mice showed a second, even more pronounced, rise of corticosterone towards the end of their subjective night (33 hours after "lights off"). A 2-way ANOVA revealed a significant difference between the two groups over the time course studied ($p=0.01$) (Fig. 4A). When we stressed the mice by transferring them into a restrainer, SCN-*Bmal1*-KD and control mice showed a similar increase of corticosterone after the first 10 min of stress. However, after 30 min of stress, SCN-*Bmal1*-KD mice displayed significantly lower corticosterone levels than control mice. Analyses of these data by 2-way ANOVA indicate a statistically significant difference between SCN-*Bmal1*-KD and control mice ($p=0.0242$) (Fig. 4B).

Discussion

In this study we investigated whether disrupting rhythms in the central SCN circadian clock alters mood-related behavior. Mechanistic connections between disturbed circadian clocks and mood regulation have been evaluated before in rodent models (7, 8, 11). However, in previous studies it was not clear whether circadian or non-circadian changes led to abnormal mood-related behavior (13). Manipulations of lighting conditions, light input pathways, or expression of genes involved in circadian rhythms always involve consequences that are independent of the actual diurnal oscillations produced by intrinsic circadian clocks. In contrast, our study provides an animal model with normally developed, anatomically intact brain and light input pathways, and intact molecular clock gene machinery in all non-SCN brain regions and peripheral tissues, under normal LD 12:12 lighting conditions. To create such a model, we performed a shRNA-induced knockdown of *Bmal1* expression restricted to the SCN. The efficiency of the knockdown was determined individually for each animal by the amplitude of PER2::LUC expression rhythms of SCN explants prepared after completion of all behavioral experiments.

Bmal1-KD SCN explants generally still showed significant circadian rhythms, but with ~80% lower amplitude and longer period compared to control SCN explants. Accordingly, SCN-*Bmal1*-KD mice still showed circadian activity rhythms in DD, but with longer free-running periods. Interestingly, many MDD patients display decreased circadian rhythm amplitude (30) and abnormally delayed melatonin (31, 32) and behavioral rhythms (33). It is well known that longer free-running period is typically associated with delayed phase of entrainment, suggesting that MDD patients may also have abnormally long circadian periods. However, the locomotor activity rhythm is just one output of the central clock in the SCN. In view of strongly attenuated SCN rhythm amplitude, it is quite possible that other SCN-regulated rhythms

are more strongly affected than locomotor activity rhythms. Furthermore, long circadian SCN period in SCN-*Bmal1*-KD mice may promote internal desynchrony among brain areas and other tissues whose clocks are genetically intact. Circadian misalignment among brain regions could contribute to the development of mood-related abnormalities (9, 28). Thus, in our mouse model, circadian rhythms in the SCN were greatly weakened and period was lengthened, but rhythms were not completely eliminated, a realistic model of the kind of disruption most likely to occur in humans.

Disrupting circadian rhythms of the central circadian pacemaker in the SCN causes several robust mood-related behavioral changes. In particular, compared to control mice injected with a scrambled sequence shRNA, SCN-*Bmal1*-KD mice exhibit increases in behavioral despair, anxiety-like behavior, and helplessness. Even before mice are exposed to the inescapable stress (IS) of the learned helplessness induction procedure, SCN-*Bmal1*-KD mice already show significantly increased immobility times in the tail suspension test, conventionally interpreted as a sign of increased behavioral despair (although this interpretation is controversial) (23, 34). In addition, disrupting central circadian rhythms leads to increased anxiety-like behavior in the light/dark box test, manifesting as avoidance of a potentially dangerous environment. Furthermore, SCN-*Bmal1*-KD mice are more helpless than control mice, showing increased latencies or failures to escape foot shock. Importantly, running wheel activity measurements and the open field test revealed that our SCN-specific *Bmal1*-KD procedure does not alter levels of general locomotor activity. Just as for behavioral despair and anxiety-like behavior, helplessness in SCN-*Bmal1*-KD mice is already present at baseline, even before they are subjected to IS training. Although exposure to IS is usually seen as being essential for "*learned* helplessness", "congenital helpless" rats have been characterized that display increased active avoidance latencies and other signs of depression-like behavior without induction by IS (35). Accordingly, SCN-*Bmal1*-KD mice represent a new genetic animal model of helplessness, despair, and anxiety.

Not all mood-related behaviors are altered in SCN-*Bmal1*-KD mice. Hedonic behavior in the sucrose preference test, spatial preference in the open field test, and aversion to eating in a novel environment are all similar in SCN-*Bmal1*-KD and control mice. This indicates that specific aspects of mood-related behavior are influenced differently by the suppression of SCN circadian rhythms.

Since the SCN is not known to be directly involved in mood regulation, it is likely that disruption of the central clock affects mood by causing disturbed circadian rhythms in downstream systems that regulate mood more directly (9). One such system is the HPA axis, which is tightly associated with both the circadian clock and mood regulation (29). In this study we show that mice with disrupted SCN rhythms have abnormally high corticosterone levels toward the end of their subjective night, manifesting as a second peak of corticosterone release in addition to the expected rise at the beginning of the subjective night. Another study investigated corticosterone levels in a different SCN clock-deficient mouse model achieved by neuron-specific knockout of *Bmal1* using Cre recombinase expressed under a *Syt10* promoter (3). In that study, performed in a light/dark cycle, corticosterone rhythms were not different in SCN clock-deficient and control mice, suggesting that the light/dark cycle may compensate for the loss of SCN rhythms by directly modulating corticosterone release (3-5). Because our experiment was carried out in constant darkness, without potential “masking” influences of light, we were able to detect more directly the impact of SCN rhythms on rhythmic release of corticosterone from the adrenals. We found that SCN-*Bmal1*-KD mice display a reduced corticosterone response to stress, suggesting an essential role of the SCN clock in this response. This blunted corticosterone response to stress could explain the helpless behavior of SCN-*Bmal1*-KD mice, as attenuated levels of corticosterone were previously associated with escape deficits in learned helplessness (36-38). Thus, low amplitude SCN rhythms may

cause changes in mood-related behavior at least in part by altering corticosterone levels at baseline and in response to stress.

Another possibility is that knockdown of the SCN central circadian pacemaker leads to disturbed rhythms in downstream brain areas that are more directly involved in mood regulation (9, 28). Such brain areas are likely to harbor less stable clocks than the SCN (39), and their circadian oscillations may therefore be extremely disturbed in the presence of low amplitude SCN rhythms. Indeed, in a recent study we found that certain brain regions implicated in mood regulation do indeed show disrupted rhythms in helpless mice (28). Most mice that become helpless in the learned helplessness procedure exhibit an absence of circadian rhythms in the nucleus accumbens and the periaqueductal gray. However, it remains to be determined whether disrupting circadian rhythms specifically in these areas, individually or in combination, is sufficient to cause changes in mood-related behavior.

Finally, we found that SCN-*Bmal1*-KD mice display increased weight gain, despite unchanged food intake. Importantly, many psychiatric disorders, including MDD, are associated with metabolic disturbances and obesity (40). Because circadian clocks control both affective and metabolic functions, we previously suggested that disturbed circadian rhythms may play an important role in mediating the comorbidity of metabolic and psychiatric disorders (40). Although our results are preliminary, they support the hypothesis that disturbed circadian rhythms lead to both mood-related and metabolic abnormalities simultaneously in SCN-*Bmal1*-KD mice.

Our data provide evidence that disturbed circadian clocks are sufficient for the development of depression-like behavior in different behavioral tests, helplessness at baseline as well as after stress, anxiety-like behavior, and weight gain. By using a mouse model with genetic disruption of circadian

rhythms specific to the SCN but normal brain development and anatomy and a normal light/dark environment, we can exclude pleiotropic effects of clock genes in mood-regulating systems, loss of neuronal connections, and light-related factors in the development of mood-related behavioral abnormalities. Our data suggest that disturbed clocks impact the stress system, and probably also circadian oscillators in mood-regulating brain areas, which may explain the increase of helplessness, behavioral despair, and anxiety-like behavior in SCN-*Bmal1*-KD mice (Fig. 5). Future studies of non-SCN clocks in the stress system and other brain regions may provide more targeted chronotherapies for patients with mood disorders.

Acknowledgement

Supported by a Veterans Affairs Merit Award (1I01BX001146) and a NARSAD Young Investigator Award to David K. Welsh. We thank Sandra Braun and Alan Turken from Dr. Richard Hauger's lab (Veterans Affairs San Diego Healthcare System) for their help with corticosterone measurements.

Financial Disclosures

The authors report no biomedical financial interests or potential conflicts of interest.

References

1. Welsh DK, Takahashi JS, Kay SA (2010): Suprachiasmatic nucleus: cell autonomy and network properties. *Annual review of physiology*. 72:551-577.

2. Hattar S, Kumar M, Park A, Tong P, Tung J, Yau KW, et al. (2006): Central projections of melanopsin-expressing retinal ganglion cells in the mouse. *The Journal of comparative neurology*. 497:326-349.

3. Husse J, Leliavski A, Tsang AH, Oster H, Eichele G (2014): The light-dark cycle controls peripheral rhythmicity in mice with a genetically ablated suprachiasmatic nucleus clock. *FASEB journal : official publication of the Federation of American Societies for Experimental Biology*. 28:4950-4960.

4. Kiessling S, Sollars PJ, Pickard GE (2014): Light stimulates the mouse adrenal through a retinohypothalamic pathway independent of an effect on the clock in the suprachiasmatic nucleus. *PloS one*. 9:e92959.

5. Oster H, Damerow S, Kiessling S, Jakubcakova V, Abraham D, Tian J, et al. (2006): The circadian rhythm of glucocorticoids is regulated by a gating mechanism residing in the adrenal cortical clock. *Cell metabolism*. 4:163-173.

6. Ishida A, Mutoh T, Ueyama T, Bando H, Masubuchi S, Nakahara D, et al. (2005): Light activates the adrenal gland: timing of gene expression and glucocorticoid release. *Cell metabolism*. 2:297-307.

7. Boyce P, Barriball E (2010): Circadian rhythms and depression. *Australian family physician*. 39:307-310.

8. Schnell A, Albrecht U, Sandrelli F (2014): Rhythm and mood: relationships between the circadian clock and mood-related behavior. *Behavioral neuroscience*. 128:326-343.

9. McCarthy MJ, Welsh DK (2012): Cellular circadian clocks in mood disorders. *Journal of biological rhythms*. 27:339-352.

10. McClung CA (2007): Circadian genes, rhythms and the biology of mood disorders. *Pharmacology & therapeutics*. 114:222-232.

11. Kronfeld-Schor N, Einat H (2012): Circadian rhythms and depression: human psychopathology and animal models. *Neuropharmacology*. 62:101-114.

12. Li JZ, Bunney BG, Meng F, Hagenauer MH, Walsh DM, Vawter MP, et al. (2013): Circadian patterns of gene expression in the human brain and disruption in major depressive disorder. *Proceedings of the National Academy of Sciences of the United States of America*. 110:9950-9955.

13. Landgraf D, McCarthy MJ, Welsh DK (2014): The role of the circadian clock in animal models of mood disorders. *Behavioral neuroscience*. 128:344-359.

14. Ushijima K, Morikawa T, To H, Higuchi S, Ohdo S (2006): Chronobiological disturbances with hyperthermia and hypercortisolism induced by chronic mild stress in rats. *Behavioural brain research*. 173:326-330.

15. Gorka Z, Moryl E, Papp M (1996): Effect of chronic mild stress on circadian rhythms in the locomotor activity in rats. *Pharmacology, biochemistry, and behavior*. 54:229-234.

16. Logan RW, Edgar N, Gillman AG, Hoffman D, Zhu X, McClung CA (2015): Chronic Stress Induces Brain Region-Specific Alterations of Molecular Rhythms that Correlate with Depression-like Behavior in Mice. *Biological psychiatry*.

17. Savalli G, Diao W, Schulz S, Todtova K, Pollak DD (2015): Diurnal oscillation of amygdala clock gene expression and loss of synchrony in a mouse model of depression. *Int J Neuropsychopharmacol*. 18.

18. Rosenberg R, Doghramji PP (2011): Is shift work making your patient sick? Emerging theories and therapies for treating shift work disorder. *Postgraduate medicine*. 123:106-115.

19. Monje FJ, Cabatic M, Divisch I, Kim EJ, Herkner KR, Binder BR, et al. (2011): Constant darkness induces IL-6-dependent depression-like behavior through the NF-kappaB signaling pathway. *The Journal of neuroscience : the official journal of the Society for Neuroscience*. 31:9075-9083.

20. Dulcis D, Jamshidi P, Leutgeb S, Spitzer NC (2013): Neurotransmitter switching in the adult brain regulates behavior. *Science*. 340:449-453.

21. Gonzalez MM, Aston-Jones G (2008): Light deprivation damages monoamine neurons and produces a depressive behavioral phenotype in rats. *Proceedings of the National Academy of Sciences of the United States of America*. 105:4898-4903.

22. Tataroglu O, Aksoy A, Yilmaz A, Canbeyli R (2004): Effect of lesioning the suprachiasmatic nuclei on behavioral despair in rats. *Brain research*. 1001:118-124.

23. Cryan JF, Mombereau C (2004): In search of a depressed mouse: utility of models for studying depression-related behavior in genetically modified mice. *Molecular psychiatry*. 9:326-357.

24. Fernandez F, Lu D, Ha P, Costacurta P, Chavez R, Heller HC, et al. (2014): Circadian rhythm. Dysrhythmia in the suprachiasmatic nucleus inhibits memory processing. *Science*. 346:854-857.

25. Yoo SH, Yamazaki S, Lowrey PL, Shimomura K, Ko CH, Buhr ED, et al. (2004): PERIOD2::LUCIFERASE real-time reporting of circadian dynamics reveals persistent circadian oscillations in mouse peripheral tissues. *Proceedings of the National Academy of Sciences of the United States of America*. 101:5339-5346.

26. Welsh DK, Yoo SH, Liu AC, Takahashi JS, Kay SA (2004): Bioluminescence imaging of individual fibroblasts reveals persistent, independently phased circadian rhythms of clock gene expression. *Current biology : CB*. 14:2289-2295.

27. Landgraf D, Long J, Der-Avakian A, Streets M, Welsh DK (2015): Dissociation of learned helplessness and fear conditioning in mice: a mouse model of depression. *PloS one*. 10:e0125892.

28. Landgraf D, Long JE, Welsh DK (2015): Depression-Like Behavior in Mice is Associated with Disrupted Circadian Rhythms in Nucleus Accumbens and Periaqueductal Gray. *Eur J Neurosci*. Under revision.

29. Landgraf D, McCarthy MJ, Welsh DK (2014): Circadian clock and stress interactions in the molecular biology of psychiatric disorders. *Current psychiatry reports*. 16:483.

30. Souetre E, Salvati E, Belugou JL, Pringuey D, Candito M, Krebs B, et al. (1989): Circadian rhythms in depression and recovery: evidence for blunted amplitude as the main chronobiological abnormality. *Psychiatry research*. 28:263-278.

31. Buckley TM, Schatzberg AF (2010): A pilot study of the phase angle between cortisol and melatonin in major depression - a potential biomarker? *Journal of psychiatric research*. 44:69-74.

32. Emens J, Lewy A, Kinzie JM, Arntz D, Rough J (2009): Circadian misalignment in major depressive disorder. *Psychiatry research*. 168:259-261.

33. Kitamura S, Hida A, Watanabe M, Enomoto M, Aritake-Okada S, Moriguchi Y, et al. (2010): Evening preference is related to the incidence of depressive states independent of sleep-wake conditions. *Chronobiology international*. 27:1797-1812.

34. Pollak DD, Rey CE, Monje FJ (2010): Rodent models in depression research: classical strategies and new directions. *Annals of medicine*. 42:252-264.

35. Henn FA, Vollmayr B (2005): Stress models of depression: forming genetically vulnerable strains. *Neuroscience and biobehavioral reviews*. 29:799-804.

36. Edwards E, Harkins K, Wright G, Henn F (1990): Effects of bilateral adrenalectomy on the induction of learned helplessness behavior. *Neuropsychopharmacology : official publication of the American College of Neuropsychopharmacology*. 3:109-114.

37. Chover-Gonzalez AJ, Jessop DS, Tejedor-Real P, Gibert-Rahola J, Harbuz MS (2000): Onset and severity of inflammation in rats exposed to the learned helplessness paradigm. *Rheumatology (Oxford)*. 39:764-771.

38. Toloknov AV, Vvedenskaia OV, Bol'shakova TD, Buniatian AF, Khitrov NK, Fisenko VP (1999): Blood corticosterone and resistance to hypoxia during operant learning and development of learned helplessness. *Biulleten' eksperimental'noi biologii i meditsiny*. 128:29-31.

39. Liu AC, Welsh DK, Ko CH, Tran HG, Zhang EE, Priest AA, et al. (2007): Intercellular coupling confers robustness against mutations in the SCN circadian clock network. *Cell*. 129:605-616.

40. Barandas R, Landgraf D, McCarthy MJ, Welsh DK (2015): Circadian Clocks as Modulators of Metabolic Comorbidity in Psychiatric Disorders. *Current psychiatry reports*. 17:98.

Figure legends

Fig. 1: Knockdown of *Bmal1* expression abolishes circadian rhythms in SCN. (A) AAV expression constructs encoding GFP and shRNAs targeting *Bmal1*. (B) SCNs of mice were injected with AAVs carrying *Bmal1*-KD or scrambled shRNA sequences, as well as a GFP reporter. Fluorescence images of representative fields show GFP expression marking cell nuclei by Hoechst staining (blue), transduced cells marked by GFP (green), and BMAL1 protein levels by immunolabeling (red) from SCN-Bmal1-KD and control mice. The overlay shows that most *Bmal1*-shRNA transfected cells show reduced BMAL1 levels. (C) Immunofluorescence labeling reveals a ~60% reduction of BMAL1 protein levels in the SCN of mice injected with *Bmal1*-shRNA relative to control mice. Data are shown as mean ± SEM; *$p \leq 0.05$, $t_4=3.657$ (Student's t-test); n=3. (D) After AAV injections and subsequent behavioral experiments, coronal organotypic SCN explants of all mice were prepared (left) to confirm correct location of injections based on GFP expression patterns (right) and to determine the efficiency of *Bmal1* knockdown based on amplitude of PER2::LUC rhythms. (E) On average, knockdown of *Bmal1* expression reduces PER2::LUC rhythm amplitude by ~80% and significantly lengthens PER2::LUC circadian rhythm period. SCN explants from mice that received scrambled sequence control injections show PER2::LUC rhythms similar in amplitude to those from untreated mice. Amplitude data are shown as mean ± SEM; $F_{2,26}=15.98$ (1-way ANOVA with Bonferroni post test; ***$p \leq 0.001$); n=9-10. Period data are shown as mean ± SEM; $t_{17}=2.279$ (Student's t-test); n=9-10. (F) Representative PER2::LUC rhythms of SCN explants injected with AAV particles encoding scrambled shRNA sequences (left) and shRNA targeting *Bmal1* RNA (right). (G) Representative actograms showing wheel-running activity during entrainment in an LD 12:12 light/dark cycle and subsequent constant darkness. Gray shading represents times of darkness. (H) SCN-*Bmal1*-KD mice display longer circadian free-running periods of locomotor activity in constant darkness. Data are shown as mean ± SEM; **$p \leq 0.01$, $t_{11}=4.104$ (Student's t-test); scrambled: n=8, SCN-*Bmal1*-KD: n=5.

Fig. 2: Disruption of circadian rhythms in the SCN leads to increased helplessness, despair, weight gain, and anxiety-related behavior. (A) In the LHelp paradigm, *Bmal1*-KD in SCN increases escape latency times (left) and number of escape failures (right). Data are shown as mean ± SEM; *p ≤ 0.05, **p ≤ 0.01; latency time: t_{17}=2.997, escape failures: t_{17}=2.801 (Student's t-test); n=9-10. (B) In the TST, *Bmal1*-KD in SCN increases immobility time. Data are shown as mean ± SEM; **p ≤ 0.01; t_{25}=3.067 (Student's t-test); n=12-15. (C) During the five weeks after AAV injection, SCN-*Bmal1*-KD mice gain significantly more weight than control mice. Data are shown as mean ± SEM; *p ≤ 0.05; t_{16}=2.693 (Student's t-test); n=8-10. (D) In the sucrose preference test, *Bmal1*-KD in SCN has no significant impact on preference for sweet water. Data are shown as mean ± SEM; Interaction: $F_{10,120}$=1.189, p=0.352; Time: $F_{1,120}$=1.355, p=0.2093; Genotype: $F_{10,120}$=0.8537, p=0.3737; post hoc test: not significant (2-way repeated measures ANOVA with Bonferroni post test); n=9-10. (E) Suppression of SCN rhythms does not change the aversion to eating in a novel environment (expressed as latency to begin eating) or total food intake (expressed per 10 min during the test or per day). Data are shown as mean ± SEM; not significant; latency time: t_{11}=0.1600, food intake in novel environment: t_{11}=0.9643, daily food intake: t_{11}=1.173 (Student's t-test); n=5-8. (F) SCN-*Bmal1*-KD mice spend significantly less time in the light compartment of a light/dark box, conventionally interpreted as an increase in anxiety-related behavior. Data are shown as mean ± SEM; *p ≤ 0.05; t_{11}=2.430 (Student's t-test); n=5-8. (G) In the open field test, *Bmal1*-KD in SCN does not alter spatial preference or total activity. Data are shown as mean ± SEM; not significant; time in center: t_{15}=0.5319, immobility time: t_{15}=0.4397 (Student's t-test); n=7-10.

Fig. 3: Disruption of SCN circadian clock function leads to a state of helplessness as manifested by decreased active avoidance of foot shock. Even without previous exposure to inescapable stress, *Bmal1-KD* in SCN leads to higher escape latency times (left) and increased numbers of escape failures during

testing in the LHelp shuttle boxes. Data are shown as mean ± SEM; *p ≤ 0.05, **p ≤ 0.01; latency time: t_8=4.069, escape failures: t_8=3.301 (Student's t-test); n=5.

Fig. 4: SCN-*Bmal1*-KD mice have altered stress hormone function. (A) Circadian patterns of corticosterone release in SCN-*Bmal1*-KD and control mice kept in constant darkness. In addition to the normal increase of corticosterone at the beginning of the subjective night (25 hours after "lights off"), SCN-*Bmal1*-KD mice have a second corticosterone peak at the end of subjective night (33 hours after "lights off"). Data are shown as mean ± SEM and Fourier-curve fits with 2 harmonics; Interaction: $F_{5,70}$=3.279, p=0.0102; Stress: $F_{1,70}$=18.45, p=<0.0001; Genotype: $F_{5,70}$=0.01066, p=0.9192; post hoc test: *p ≤ 0.05 (2-way repeated measures ANOVA with Bonferroni post test); n=8. (B) Corticosterone release of SCN-*Bmal1*-KD and control mice in response to acute 30 min restraint stress. SCN-*Bmal1*-KD mice show an attenuated corticosterone increase. Data are shown as mean ± SEM; Interaction: $F_{3,39}$=1.23, p=0.3101; Stress: $F_{1,39}$=38.45, p=<0.0001; Genotype: $F_{3,39}$=6.500, p=0.0242; post hoc test: *p ≤ 0.05 (2-way repeated measures ANOVA with Bonferroni post test); n=7-8.

Fig. 5: Alternative models of how disruption of the clock network could lead to abnormal mood phenotypes. (A) In healthy subjects, the clock network is intact and synchronized (green), including the SCN master pacemaker (big clock) and various peripheral clocks, including brain clocks and clocks in other tissues like the adrenal (small clocks). (B) However, if the SCN master pacemaker is rendered non-rhythmic (red), all downstream peripheral clocks, including those important for mood regulation, are disturbed as well, because their component cellular circadian oscillators are no longer synchronized by the SCN. This leads to abnormal mood. (C) Alternatively, an abnormal mood phenotype may occur when only a subset of peripheral clocks is disturbed. This may involve loss of rhythms due to asynchronous component cellular oscillators (red) or loss of synchronization with other tissues, e.g. in adrenal (yellow).

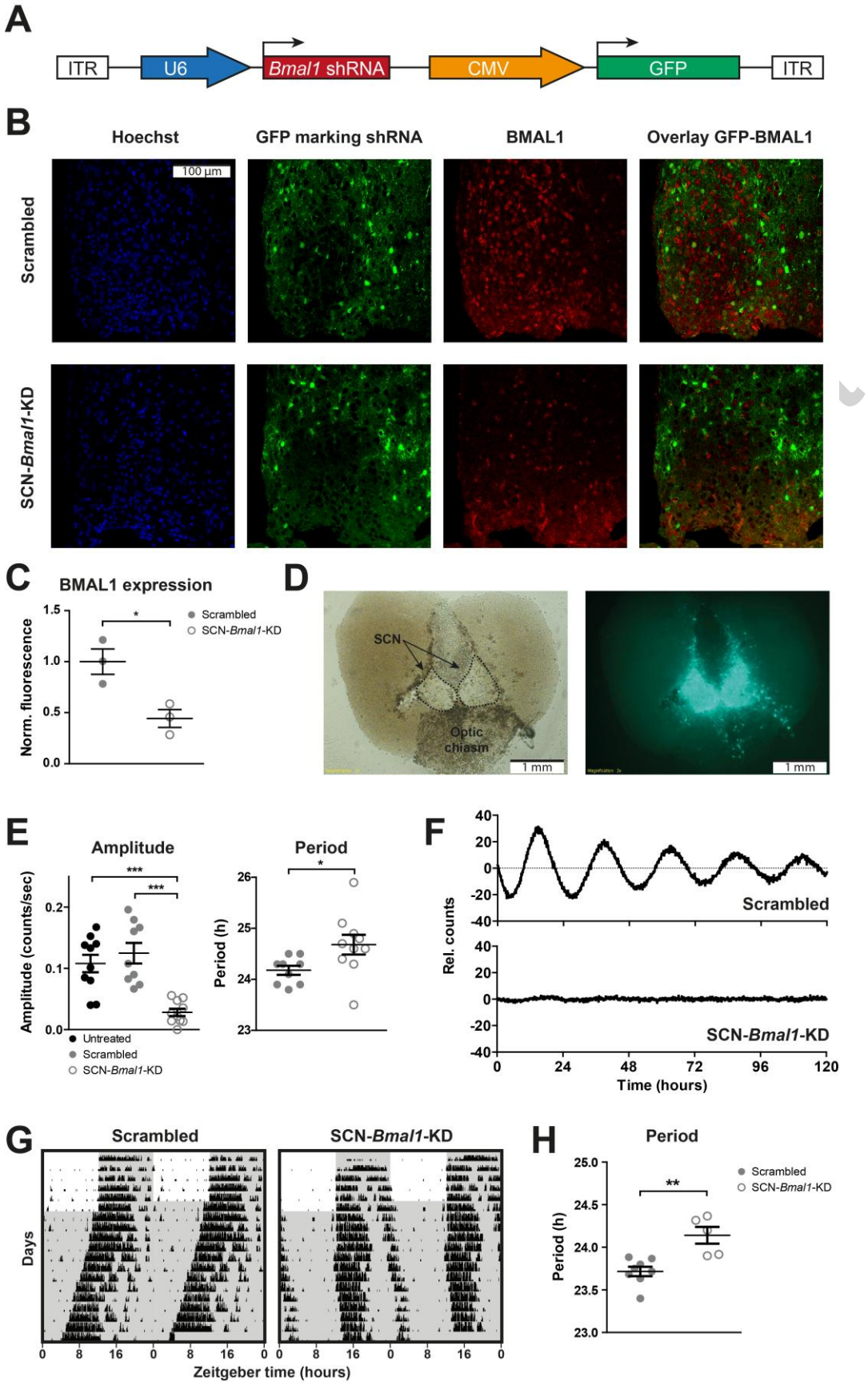
A
ITR
U6
Bmal1 shRNA
CMV
GFP
ITR
B
Hoechst
GFP marking shRNA
BMAL1
Overlay GFP-BMAL1
100 µm
Scrambled
SCN-Bmal1-KD
C
BMAL1 expression
Norm. fluorescence
Scrambled
SCN-Bmal1-KD
D
SCN
Optic chiasm
1 mm
1 mm
E
Amplitude
Amplitude (counts/sec)
Period
Period (h)
Untreated
Scrambled
SCN-Bmal1-KD
F
Rel. counts
Scrambled
SCN-Bmal1-KD
Time (hours)
G
Scrambled
SCN-Bmal1-KD
Days
Zeitgeber time (hours)
H
Period
Period (h)
Scrambled
SCN-Bmal1-KD

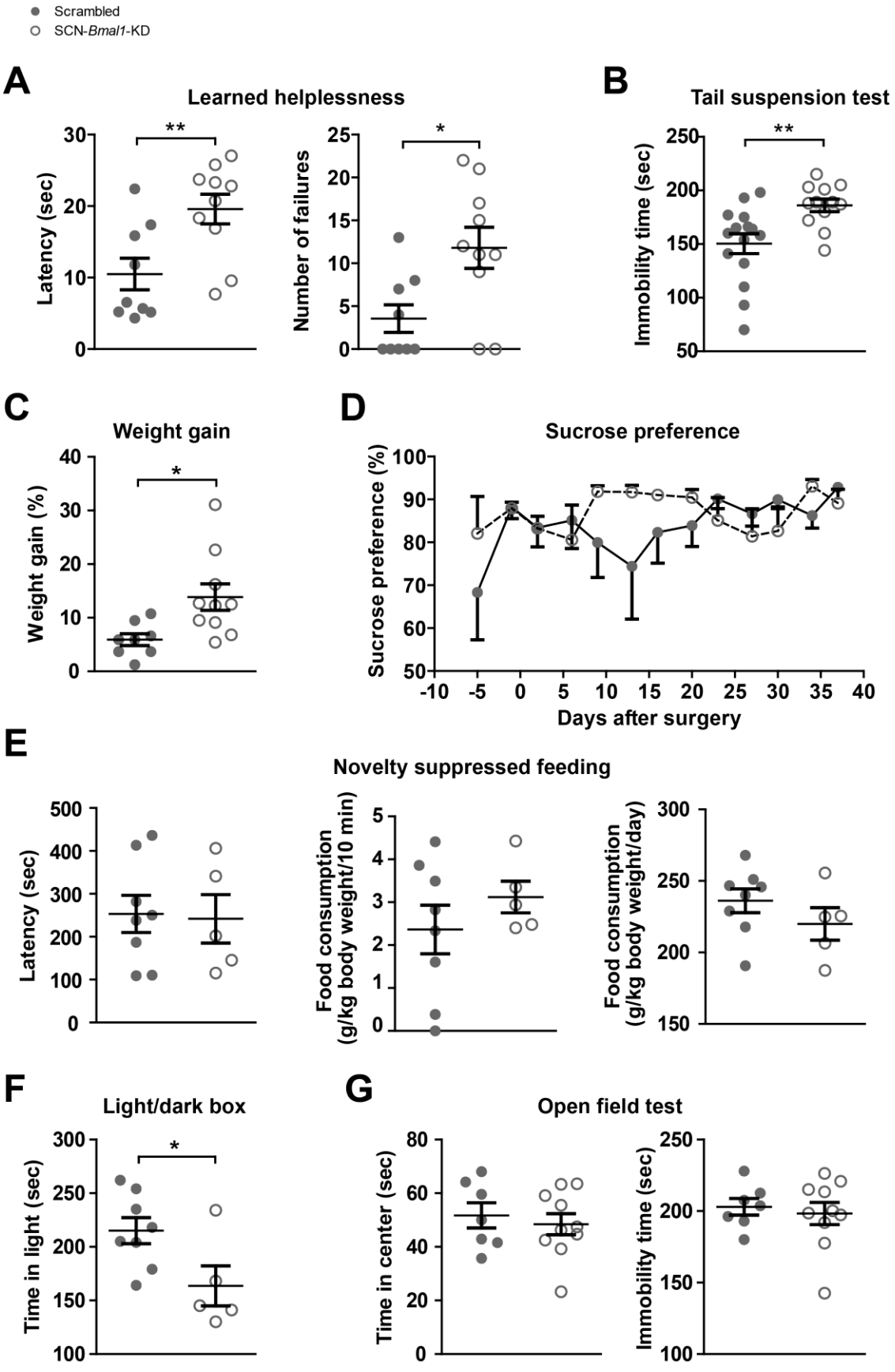
Scrambled
SCN-Bmal1-KD
A
Learned helplessness
Latency (sec)
Number of failures
B
Tail suspension test
Immobility time (sec)
C
Weight gain
Weight gain (%)
D
Sucrose preference
Sucrose preference (%)
Days after surgery
E
Novelty suppressed feeding
Latency (sec)
Food consumption (g/kg body weight/10 min)
Food consumption (g/kg body weight/day)
F
Light/dark box
Time in light (sec)
G
Open field test
Time in center (sec)
Immobility time (sec)